DOI 10.1007/s11148-019-00330-0
Refractories and Industrial Ceramics *Vol. 60, No. 2, July, 2019*

EVALUATION OF THE CRACK RESISTANCE OF REACTIVE SINTERED COMPOSITE BORON CARBIDE-BASED MATERIALS

S. N. Perevislov[1,2]

Translated from *Novye Ogneupory*, No. 3, pp. 49 – 54, March 2019.

Original article submitted December 8, 2018.

The results of studying the crack resistance of reaction-sintered B_4C–SiC composite materials impregnated with liquid silicon with identification and fracture methods are presented. With an increase in the amount of B_4C in the reaction-sintered material, its fragility increases. The crack resistance of the material can be increased from 3.40 to 4.02 $MPa \cdot m^{1/2}$ (when tested by different methods) by adding to the composite material up to 30 wt.% SiC. The material is destroyed mainly by the intercrystalline (intergranular) mechanism. Ceramics containing more than 90 wt.% B_4C, is partially destroyed by the transcrystalline mechanism.

Keywords: boron carbide, silicon carbide, reaction sintering, siliconization, crack resistance, physical and mechanical properties, material destruction.

INTRODUCTION

Boron carbide is a unique material that combines high mechanical properties (E_{elast}450 GPa, $H_{\text{m}} = 49$ GPa), low density ($\rho = 2.51$ g/cm^3) and TCLE (4.5×10^{-6} K^{-1}), while also having good wear resistance. The properties of materials based on B_4C allow them to be used as lining elements for protecting mills, abrasive materials, armor plates, etc. [1]. Most often, materials based on B_4C are obtained by the method of hot pressing [1, 2] with 1 – 3 wt.% B + C, Al + C, B_4C or other additives. The mechanical properties of such materials are optimal: $\sigma_{\text{fl}} = 450 - 470$ MPa, $K_{\text{Ic}} = 6.0 - 6.5$ MPa·m$^{1/2}$, $HV = 38 - 40$ GPa [1]. However, despite the great advantages of hot-pressed materials, the hot-pressing method itself has several disadvantages, in particular, low productivity, high energy consumption, the use of expensive tooling – high-density graphite, the inability to produce materials of complex shape without additional diamond processing. This limits the widespread use of hot pressing and makes it necessary to search for alternative ways to obtain materials based on B_4C.

The method of reaction sintering by impregnating a porous preform consisting of particles of B_4C and soot or B_4C, SiC and soot with liquid silicon to obtain a monolithic material [3 – 8] by analogy with reaction-sintered (siliconized) silicon carbide [9, 10] has been undergoing rapid development in the recent years. Some of the disadvantages of such materials include poor mechanical characteristics (compared to hot-pressed B_4C), lower wear resistance, and large amounts (10 – 15 vol.%) of residual silicon in the composition of the final material, which increases its fragility. Nevertheless, the high productivity of the reaction sintering method and the possibility of obtaining materials of complex geometric shape attract close attention of researchers to boron carbide obtained by reaction sintering.

The crack resistance of $K_{\text{I}c}$, like other mechanical properties of ceramic materials, is largely determined by the microstructure, the main indicators of which are the number and size of pores, the size of the grains of the main phase (boron carbide), the presence of impurities and other phases. The content, size and shape of pores, the size of B_4C grains depend on the conditions of its production, and the indicators of strength properties (flexural and compression strength) monotonically deteriorate with increasing porosity and grain size [11, 12]. To determine the K_{Ic} of ceramic materials, the most commonly used tests are the Vickers hardness test [13] and the test for fracture of notched samples [14, 15]. How-

---

[1] I. V. Grebenshchikov Institute of Silicate Chemistry of the Russian Academy of Sciences, St. Petersburg, Russia.

[2] perevislov@mail.ru

ever, the Vickers hardness method does not allow to determining the crack resistance of porous materials. Despite the fact that in the literature there are data on the crack resistance of B_4C obtained by both methods [16 – 18], there is no information on the influence of structural factors on the crack resistance of reaction-sintered B_4C.

The purpose of this work is to study the crack resistance of the reaction-sintered material based on B_4C, depending on the initial content of B_4C powder.

MATERIALS AND RESEARCH METHODS

The starting materials were B_4C powder with $d_{0.5}$ of 42.0 microns and M5 SiC with $d_{0.5}$ of 3.7 μm, grade K-354 technical carbon black, and Kr00 grade silicon crushed to $d_{0.5}$ of 1.0 μm. The compositions of the materials are given in Table 1. The initial powders were mixed dry in a drum mixer for 20 hr, plasticized with a 2% aqueous solution of an organic binder and granulated through a 100 μm mesh. Samples with dimensions 60 × 60 × 10 mm were pressed from mixtures by semi-dry molding under pressure of 100 MPa, dried at 110 – 120°C for 5 h, and impregnated with liquid silicon by soaking. Next, the samples were placed in graphite containers on graphitized paper pre-lubricated with boron nitride (*h*-BN) to prevent adhesion of samples to the container due to liquid silicon.

Based on parameters for molded $SiC^I + C$ preforms ($\rho = 2.20 – 2.22$ g/cm^3, corresponding to a porosity $P = 31.0 – 31.5\%$) of reaction-sintered silicon carbide, it was shown in [19] that it is possible to calculate the density of preforms molded from materials based on boron carbide ($B_4C + C$ and $B_4C + SiC^I + C$) that is optimal for the siliconization process, and hence the theoretical density of the reaction-sintered materials based on B_4C (see Table 1), provided the following reactions take place:

$$C\ (s) + Si\ (l) \rightarrow SiC^{II}\ (s), \quad (1)$$

$$3B_4C\ (s) + Si\ (l) \rightarrow SiC^{II}\ (s) + B_{12}(C, Si, B)_3. \quad (2)$$

TABLE 1. Initial Composition of Sample Preforms Based on B_4C

Composition number	Content in the preform, wt.%			Theoretical density of sintered materials ρ_{teor}, %
	B_4C	SiC	carbon	
1	100	—	—	2.53
2	95	—	5	2.58
3	90	—	10	2.64
4	85	—	15	2.73
5	75	10	15	2.78
6	65	20	15	2.83
7	55	30	15	2.88

Thus, for the material of compositions 2 and 7, the density of preforms ρ_{prf} is estimated at 1.68 – 1.70 and 1.78 – 1.80 g/cm^3. Due to the high probability of cracking of the preforms on impregnation with an excess amount of silicon, as well as to reduce the dissolution of B_4C grains in liquid silicon melt and the formation of the negative phase $B_{12}(C, Si, B)_3$, materials are molded at a density of 0.80 – 0.85 of the maximum ρ_{prf}. The material densities of the obtained preforms of compositions 2 and 8 were ρ_{prf} 1.44 g/cm^3 ($P = 44.5\%$) and 1.53 g/cm^3 ($P = 46\%$). Samples were covered with lump silicon 4 – 5 mm in size in the amount of 0.70 – 0.72 by weight of the preform and sintered in a vacuum furnace with graphite heaters and lined with graphite at 1600°C for 10 min in a vacuum. The excess silicon on the surface of the samples after siliconization was removed by sandblasting.

The density and porosity of the sintered specimens were determined by hydrostatic weighing. The relative density was calculated from the theoretical density. The microstructure of the samples was examined on a Techno Meiji IM 7200 optical microscope. The elastic modulus was determined dynamically on a ZVUK-230 instrument, measuring the resonant frequency of longitudinal vibrations. Vickers hardness was determined by measuring the diagonal length of the Vickers pyramid imprint. X-ray diffraction analysis was performed on the Rigaku Smartlab 3 instrument. The crack resistance of materials based on B_4C was estimated from the K_{Ic} value, which was determined in two ways:

1) by the indentation (Vickers pyramid imprint) method (Fig. 1*a*), measuring the length of cracks emanating from the base of the Vickers pyramid, on the TP-7r-1 hardness meter with a load of 19.6 N. Crack resistance was calculated by the equations:

$$K_{Ic} = 0.018 \times (P/c^{1.5}) \times (E_{elast}/HV)^{0.5}, \quad (3)$$

$$K_{Ic} = 0.073 \times P/c^{1.5}, \quad (4)$$

where P is the applied load; c is the average half-length of a crack; E_{elast} is the modulus of elasticity; HV is the Vickers hardness;

2) by the three-point bending test (Fig. 1*b*) of samples notched by the electric-spark method to a depth of 1/3 of the height (notch width 0.3 mm). The speed of movement of the traverse load was 0.2 mm/min. Crack resistance was calculated by the equation:

$$K_{Ic} = ((3P \times L \times c^{1/2})/(2b \times h^2)) \times 1.93 - 3.07 \times (c/h) + 14.53 \times (c/h)^2 - 25.1 \times (c/h)^3 + 25.8 \times (c/h)^4, \quad (5)$$

where L is the distance between supports; b and h are the width and height of the sample; c is the length of the initial crack (notch).

For each material composition based on B_4C, 5 – 6 samples were tested; the relative error of determination of K_{Ic} did not exceed 10%. Research equipment was provided by the

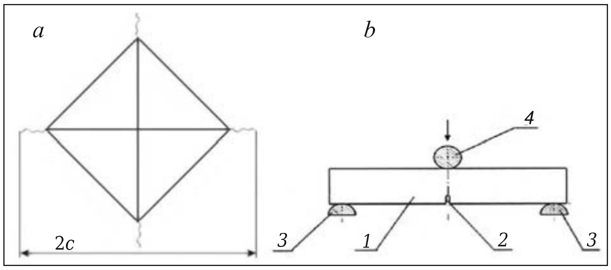

Fig. 1. A schematic representation of the Vickers pyramid imprint in the determination of K_{Ic} by the methods of indentation (*a*) and fracture (*b*): *c*) the average half-length of the crack; *1*) ceramic sample; *2*) V-shaped notch; *3*) lower supports; *4*) loading traverse.

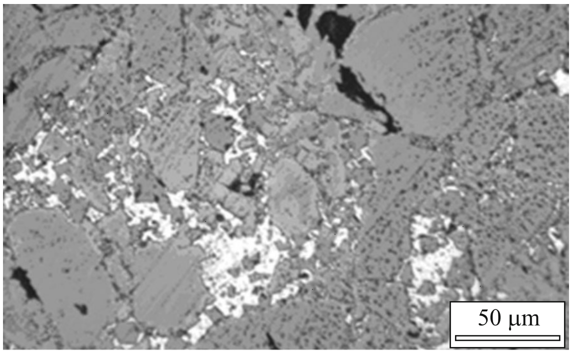

Fig. 2. Microstructure of reaction-sintered B_4C of composition 1.

St. Petersburg State Institute of Technology and Engineering (TU).

RESULTS AND DISCUSSION

In the production of the reaction-sintered silicon carbide materials, silicon dissolves carbon while being absorbed into the porous preform, saturating the melt to the solubility limit, and subsequently a secondary crystalline silicon carbide (SiC^{II}) of the cubic modification (β-SiC) crystallizes from the melt on the surface of the primary grains (SiC^{I}) [20 – 22]. In the reaction-sintered material based on B_4C, in addition to these phases, there is a phase of a solid solution of silicon in boron carbide — $B_{12}(C, Si, B)_3$, which crystallizes on the B_4C grains in dense ring-like layers, known as "core-shell" structure [23, 24]. The grains of the initial boron carbide are the "core", and the "shell" is the solid solution of silicon in boron carbide, interconnected in a three-dimensional matrix (Fig. 2). The dense phase $B_{12}(C,Si,B)_3$ prevents silicon from moving deep into the porous preform, therefore, reaction-sintered B_4C is characterized by increased porosity (Table 2) compared to reaction-sintered SiC [25].

Due to the high viscosity of the melt, materials without the addition of SiC cannot be consolidated to the maximum density ($P = 1.5 – 3.7\%$, compositions 1 – 4). In the compositions without the addition of carbon, its only source is B_4C, which gives off carbon on dissolution in the silicon melt, increasing the solid solution content, impairing the impregnation of the porous preform. Therefore, the material of composition 1 has the highest porosity ($P = (96.3 \pm 0.1)\%$, see Table 2). With the introduction of up to 15 wt.% carbon into the material, the amount of viscous melt of composition $B_{12}(C,Si,B)_3$ decreases, increasing the impregnation of porous preforms and, consequently, their density (see Table 2). Introduction of up to 30 wt.% of SiC reduces the viscosity of the silicon melt, allowing for maximum compaction of the B_4C–SiC composite ($\rho_{rel} = (96.3 \pm 0.1)\%$, $P = (0.9 \pm 0.1)\%$). Porosity strongly affects a number of mechanical characteristics, E_{elast} in particular, the value of which is low when the density of materials without silicon carbide is low (compounds 1 – 4) (see Table 2). With an increase in the density of the composite B_4C–SiC (compositions 5 – 7), E_{elast} increases, reaching the maximum value in the material of composition 7, where $E_{elast} = (345 \pm 5)$ GPa. The hardness of a composite material depends on the hardness of its phases. Boron carbide has maximum hardness; when less solid silicon carbide is introduced into the material, the total hardness decreases to $HV = (27.8 \pm 0.1)$ GPa (see Table 2, composition 7).

The dependence of K_{Ic} calculated by equation (3) has a monotonic character, decreasing with increasing content of B_4C in the material (Fig. 3). The lack of carbon in compositions 1 – 3, leading to the formation of a solid solution

TABLE 2. Physical and Mechanical Properties of Composite Materials Based on B_4C.

Composition number	Density ($\rho \pm 0.02$), g/cm^3	Relative density ($\rho_{rel} \pm 0.1$), %	Porosity ($\Pi \pm 0.1$), %	Modulus of elasticity ($E_{elast} \pm 5$), GPa	Vickers hardness ($HV \pm 0.1$), GPa
1	2.44	96.3	3.7	300	35.0
2	2.51	97.1	2.9	308	33.8
3	2.58	97.8	2.2	315	33.1
4	2.69	98.5	1.5	319	32.4
5	2.75	98.8	1.2	325	29.3
6	2.80	99.0	1.0	334	28.4
7	2.85	99.1	0.9	345	27.8

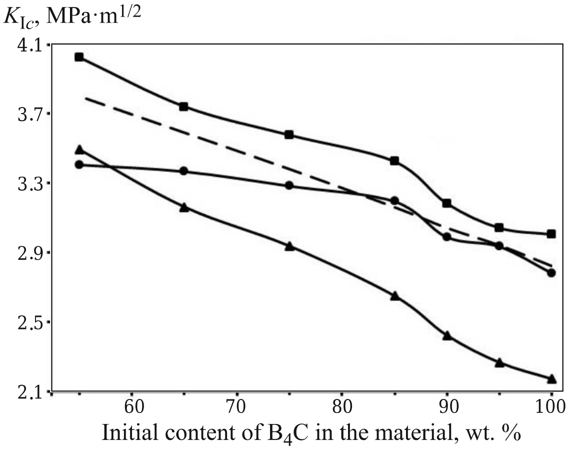

Fig. 3. The dependence of K_{Ic} of the reaction-sintered material on the initial content of B_4C in it: ▲) K_{Ic} calculated by the equation (3); ■) by the equation (4); ●) by the equation (5); - - - -) average K_{Ic} value.

$B_{12}(C,Si,B)_3$, increases the fragility of the composite material based on B_4C. Porosity in all samples (<4%) is evenly distributed and does not form clusters; it does not affect the nature of the destruction (see Fig. 2). The fractures of the specimens tested for crack resistance were subjected to detailed fractographic electron microscopic analysis (Fig. 4). In contrast to hot-pressed B_4C [26], in which the particles are contact-sintered together in a single dense monolith, in the reaction-sintered material the intergranular space is occupied by less hard silicon and secondary silicon carbide, which strongly influence the nature of the destruction. The samples are destroyed mainly in accordance with the intercrystalline (intergranular) character (see Fig. 4). Microfractures stop developing at the grain boundaries. In samples with a high content of B_4C (compounds 1 – 3), in which an annular solid solution layer with a lower hardness is formed on the B_4C grains, the fracture can destroy the grains (the transcrystalline nature of the destruction). With the introduction of up to 30 wt.% silicon carbide into the material, the values of K_{Ic} increase from (2.94 ± 0.02) to (3.49 ± 0.02) MPa·m$^{1/2}$.

The most reliable K_{Ic} values are determined by the fracture method, which makes it possible to evaluate the crack resistance of the real defect material, in contrast to the indentation method, in which high porosity does not allow qualitative measurement of K_{Ic}, and low porosity or high content of the $B_{12}(C,Si,B)_3$ solid solution phase, locally concentrated in individual zones of the sample, may not fall into the area impacted by the Vickers pyramid and artificially increase K_{Ic} values (calculated by equation (4)). In general, crack resistance determined by the indentation (calculated by equation (4)) and fracture methods has similar values (see Fig. 3). Based on the K_{Ic} values calculated using equations (4) and (5), it is possible to construct a curve of the average K_{Ic} value for reaction-sintered material based on B_4C (see Fig. 3, dashed line).

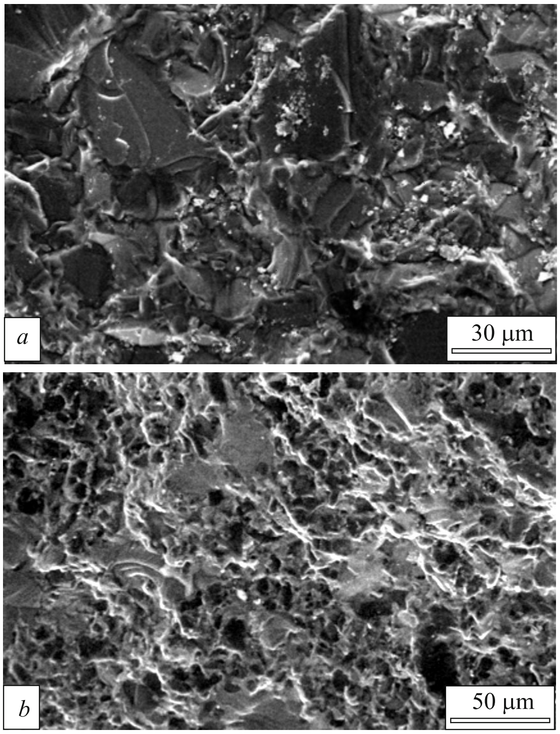

Fig. 4. Fractograms of the destruction of reaction-sintered materials based on B_4C: *a*) composition 1; *b*) composition 7.

Regardless of the method (indentation or fracture), considering or ignoring the values of E_{elast} and *HV*, conflicting K_{Ic} values were obtained, ranging from (2.17 ± 0.02) to (3.00 ± 0.02) MPa·m$^{1/2}$ (for the composition with the maximum content of B_4C), and there is a general pattern of increasing fragility of the ceramic material with an increase in the content of B_4C. The maximum values of K_{Ic} were achieved for a composite material with 30 wt.% SiC: (3.49 ± 0.02) MPa·m$^{1/2}$ when calculated according to equation (3), (4.02 ± 0.02) MPa·m$^{1/2}$ when calculated by equation (4) and (3.40 ± 0.02) MPa·m$^{1/2}$ when calculated by equation (5).

Microstresses can have a significant effect on the crack resistance of reaction-sintered B_4C. In the present work, microstresses were studied using an approximation method, by x-ray structural analysis (analyzing the ratios of the physical broadening of diffraction reflections {330} and {220}) of B_4C-based samples. This made it possible to determine $\Delta\grave{a}/a$ by the equation $\Delta\grave{a}/a = \pm\beta/(4\text{tg}\theta)$, where a is the average lattice parameter; Δa is the maximum deviation from its average value; θ is the Bragg angle. Hence, the magnitude of microstresses can be calculated by the equation $\sigma = E_{\text{elast}}(\Delta a/a)$. The microstress level σ changes with increasing porosity and increasing volumetric content of the solid solution phase, which is typical for materials with a high content of B_4C — σ = 90 – 190 MPa (for materials of compositions 1 – 3, Fig. 5). When SiC particles are added to a composite material, its σ level decreases from 35 MPa (at

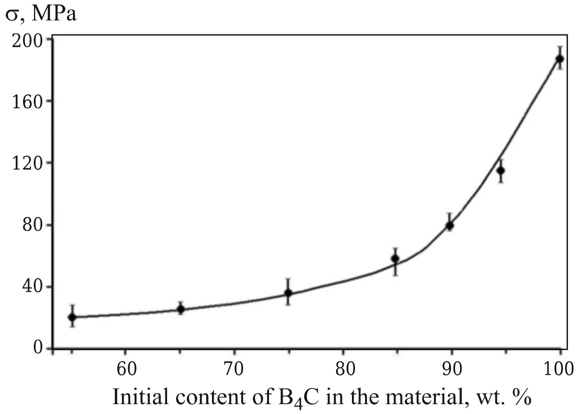

Fig. 5. Dependence of σ on the initial content of B_4C in the material.

10 wt.% SiC) to 20 MPa (at 30 wt.% SiC). The maximum value of microstresses (σ = 190 MPa) is characteristic of reaction-sintered B_4C (composition 1) with high porosity and a low elastic modulus. With increasing porosity of the reaction-sintered B_4C-based material, a high level of microstresses remains. This suggests that the presence of pores and the $B_{12}(C,Si,B)_3$ solid solution phases does not lead to relaxation of internal stresses in this material. The increase in microstresses as a function of the increase in the total porosity and the content of the $B_{12}(C,Si,B)_3$ phase in the material with the maximum amount of B_4C may be due to the heterogeneity of the medium; at the same time, the fraction of *grain – pore* boundaries becomes significant. The latter circumstance leads to an inhomogeneous distribution of thermal stresses in the material and to different conditions of their relaxation at intergrain boundaries and *grain – pore* boundaries, which can also adversely affect the level of crack resistance of the reaction-sintered B_4C-based material.

CONCLUSION

The crack resistance of the composite material B_4C–SiC, obtained by impregnating porous preforms with liquid silicon, was studied. Crack resistance was evaluated by the methods of indentation (measuring the length of cracks emanating from the base of a Vickers pyramid) and fracture (by the three-point bending test). It is shown that with an increase in the amount of B_4C, the fragility of the reaction-sintered material increases, the K_{Ic} values obtained by different methods are not high — from (2.17 ± 0.02) to (3.00 ± 0.02) MPa·$m^{1/2}$. With the introduction of up to 30 wt.% SiC into the composite material, K_{Ic} increases from (3.40 ± 0.02) to (4.02 ± 0.02) MPa·$m^{1/2}$ (when tested by different methods). The material is destroyed mainly by the intercrystalline (intergranular) mechanism, however, due to the high porosity and high amounts of the solid solution $B_{12}(C,Si,B)_3$, the material containing over 90 wt.% B_4C is destroyed partially according to the transcrystalline mechanism.

REFERENCES

1. S. N. Perevislov, P. V. Shcherbak, M. V. Tomkovich, “High-density boron carbide ceramics,” *Refract. Ind. Ceram.*, **59**(1), 32 – 36 (2018).
2. N. Cho, Z. Bao, and R. F. Speyer, “Density- and hardness-optimized pressureless sintered and post-hot isostatic pressed B_4C,” *J. Mater. Res.*, **20**(8), 2110 – 2116 (2005).
3. X. Du, Z. Zhang, Y. Wang, et al., “Hot-pressing kinetics and densification mechanisms of boron carbide,” *J. Am. Ceram. Soc.*, **98**(5), 1400 – 1406 (2015).
4. S. Hayun, N. Frage, M. P. Dariel, et al., “Dynamic response of B_4C–SiC ceramic composites,” *Ceramic Armor and Armor Systems II*, **178**, 147 – 156 (2006).
5. C. P. Zhang, H. Q. Rue, X. Y. Yue, and W. Wang, “Studies on the RBBC ceramics fabricated by reaction bonded SiC,” *Rare Metal Mat. Eng.*, **40**, 536 – 539 (2011).
6. N. A. Golubeva, L. A. Plyasunkova, I. Yu. Kelina, et al., “Study of reaction-bonded boron carbide properties,” *Refract. Ind. Ceram.*, **55**(5), 414 – 418 (2015).
7. M. P. Dariel and N. Frage, “Reaction bonded boron carbide: recent developments,” *Adv. Appl. Ceram.*, **111**(5/6), 301 – 310 (2012).
8. S. N. Perevislov, P. V. Shcherbak, and M. V. Tomkovich, “Phase composition and microstructure of reaction-bonded boron-carbide materials,” *Refract. Ind. Ceram.*, **59**(2), 179 – 183 (2018).
9. Y. Wang, S. Tan, and D. Jiang, “The effect of porous carbon preform and the infiltration process on the properties of reaction-formed SiC,” *Carbon*, **42**(8), 1833 – 1839 (2004).
10. J. C. Margiotta, D. Zhang, D. C. Nagle, and C. E. Feeser, “Formation of dense silicon carbide by liquid silicon infiltration of carbon with engineered structure,” *J. Mater. Res.*, **23**(5), 1237 – 1248 (2008).
11. P. Barick, D. C. Jana, and N. Thiyagarajan, “Effect of particle size on the mechanical properties of reaction bonded boron carbide ceramics,” *Ceram. Int.*, **39**(1), 763 – 770 (2013).
12. C. Zhang, H. Ru, H. Zong, et al., “Coarsening of boron carbide grains during the infiltration of porous boron carbide preforms by molten silicon,” *Ceram. Int.*, **42**(16), 18681 – 18691 (2016).
13. L. Sun, D. Ma, L. Wang, et al., “Determining indentation fracture toughness of ceramics by finite element method using virtual crack closure technique,” *Eng. Fract. Mech.*, **197**(6), 151 – 159 (2018).
14. F. Dai, R. Chen, and K. Xia, “A semi-circular bend technique for determining dynamic fracture toughness,” *Exp. Mech.*, **50**(6), 783 – 791 (2010).
15. A. Moradkhani, H. Baharvandi, M. Tajdari, H. Latifi, and J. Martikainen, “Determination of fracture toughness using the area of micro-crack tracks left in brittle materials by Vickers indentation test,” *J. Adv. Ceram.*, **2**(1), 87 – 102 (2013).
16. S. N. Perevislov, A. S. Lysenkov, and S. V. Vikhman, “Effect of Si additions on the microstructure and mechanical properties of hot-pressed B_4C,” *Inorg. Mater.*, **53**(4), 376 – 380 (2017).
17. X. Li, D. Jiang, J. Zhang, et al., “Reaction-bonded B_4C with high hardness,” *Int. J. Appl. Ceram. Tech.*, **13**(3), 584 – 592 (2016).

18. S. Hayun, A. Weizmann, M. P. Dariel, and N. Frage, "The effect of particle size distribution on the microstructure and the mechanical properties of boron carbide-based reaction-bonded composites," *Int. J. Appl. Ceram. Tech.*, **6**(4), 492 – 500 (2009).
19. D. D. Nesmelov and S. N. Perevislov, "Reaction sintered materials based on boron carbide and silicon carbide," *Glass Ceram.*, **71**(9/10), 313 – 319 (2015).
20. N. Frage, L. Levin, and M. P. Dariel, "The effect of the sintering atmosphere on the densification of B_4C ceramics," *J. Solid State Chem.*, **177**(2), 410 – 414 (2004).
21. S. Hayun, A. Weizmann, H. Dilman, et al., "Rim region growth and its composition in reaction bonded boron carbide composites with core-rim structure," *J. Phys.: Conference Series*, IOP Publishing, **176**(1), 1 – 7 (2009).
22. D. Mallick, T. K. Kayal, J. Ghosh, et al., "Development of multi-phase B–Si–C ceramic composite by reaction sintering," *Ceram. Int.*, **35**(4), 1667 – 1669 (2009).
23. S. N. Perevislov and D. D. Nesmelov, "Properties of SiC and Si_3N_4 based composite ceramic with nanosize component," *Glass Ceram.*, **73**(7/8), 249 – 252 (2016).
24. S. N. Perevislov, A. S. Lysenkov, D. D. Titov, M. V. Tomkovich, "Hot-pressed ceramic SiC–YAG materials," *Inorg. Mater.*, **53**(2), 206 – 211 (2017).
25. S. Xu, G. Qiao, D. Li, et al., "Reaction forming of silicon carbide ceramic using phenolic resin derived porous carbon preform," *J. Eur. Ceram. Soc.*, **29**(11), 2395 – 2402 (2009).
26. J. H. Chae, J. S. Park, J. P. Ahn, and K. H. Kim, "Mechanical properties of B_4C ceramics fabricated by a hot-press sintering," *J. Korean Ceram. Soc.*, **46**(1), 81 – 85 (2009).